



Curcumin-Loaded Iron Oxide Nanoparticles Coated with Sodium Alginate and Hydroxyapatite and Their Cytotoxic Effects Against the HT-29 and MCF-7 Cancer Cell Lines

Masoomeh Nobahari ¹, Kahin Shahanipour ^{1,*}, Soheil Fatahian ¹ and Ramesh Monajemi ²

¹Department of Biochemistry, Falavarjan Branch, Islamic Azad University, Isfahan, Iran

²Department of Biology, Falavarjan Branch, Islamic Azad University, Isfahan, Iran

*Corresponding author: Department of Biochemistry, Falavarjan Branch, Islamic Azad University, Isfahan, Iran. Email: shahanipur_k@yahoo.com

Received 2021 March 13; Revised 2021 June 06; Accepted 2021 June 09.

Abstract

Background: Curcumin, a bioactive component of *Curcuma langa*, has been investigated for its anti-proliferative effects against various cancer cell lines. Although results are very promising, the poor water solubility and low bioavailability of curcumin are its main limitations for clinical application.

Objectives: The purpose of this study was to develop a drug delivery system, consisting of hydroxyapatite (HAp) polymer and sodium alginate (NaAlg), covering the magnetic core of iron oxide nanoparticles (IONPs), and loaded with curcumin in order to enhance its bioavailability and therapeutic efficacy.

Methods: In this study, IONPs were prepared by the co-precipitation method and coated with HAp and NaAlg. The nanoparticles (NPs) were characterized by X-ray diffraction, Fourier transform infrared spectroscopy (FTIR), and electron microscopy (TEM and SEM). Encapsulation efficiency and curcumin loading rate were examined. Drug release rate was also measured in vitro at pH = 7.5 and 5.5. The toxicity of curcumin-loaded NPs and free curcumin was evaluated against HT-29 and MCF-7 cancer cells.

Results: The assessment of physicochemical characteristics showed the synthesis of spherical particles with nanometer sizes (5-7 nm) and a high encapsulation efficiency ($84.16 \pm 3.51\%$) and drug loading capacity ($21.03 \pm 0.87\%$). Maximum drug release was obtained at pH = 5.5. Iron oxide nanoparticles showed no significant cytotoxic effects. Curcumin-loaded coated IONPs showed a higher toxicity against HT-29 and MCF-7 cancer cells compared to free curcumin.

Conclusions: This in vitro study showed that the encapsulation of curcumin, as a potent herbal drug, into IONPs enhanced its bioavailability, suggesting the NPs as an efficient vehicle for targeted drug delivery in cancer treatment.

Keywords: Curcumin, Herbal Drug, HT-29, Hydroxyapatite, Iron Oxide Nanoparticles, MCF-7

1. Background

Colon cancer is the third leading cause of cancer-related deaths in the United States. Globally, it is the fourth leading cause of death among all cancers (1, 2). Breast cancer is considered the second cause of mortality in women worldwide (3). Surgery, chemotherapy, radiotherapy, immunotherapy, and hormone therapy are the main tools of cancer treatment; however, they show considerable adverse effects (4). Conventional chemotherapy bears side effects due to non-specific effects on normal tissues and the development of multidrug resistance in tumors (5). To overcome these problems, various plant-derived anti-cancer agents are available for clinical use owing to their diverse biological functions, as well as minimal side effects on normal tissues (6). Curcumin, a flavonoid, is ex-

tracted from the rhizomes of *Curcuma langa* and shows anti-oxidative and anti-inflammatory properties, as well as anti-proliferative effects against several cancer cells (7). However, its limited systemic bioavailability restricts its application as an oral therapeutic agent. To address this limitation, nanoparticulated-drug delivery systems have been widely used in order to deliver anti-cancer agents to tumors. Iron oxide nanoparticles (IONPs) have received great attention due to their ability to carry hydrophobic drugs, excellent biodegradability and biocompatibility, and a controlled drug release profile (8, 9).

In the field of cancer therapy, drug delivery systems increase the effectiveness of drugs. Targeted drug delivery systems are generally referred to as carriers capable of binding to or holding and carrying drugs in the

body. Nanostructures can penetrate into cancerous tissues, specifically through either passive (such as enhanced permeability and the retention effect) or active (for example by binding to ligands such as small molecules, peptides, or antibodies) transport systems (10, 11). However, agglomeration has limited the application of these nanoparticles (12), which has been resolved using surface functionalizing compounds, including sodium alginate (NaAlg) and hydroxy apatite (HAp). These compounds, as natural inorganic materials, present excellent and favorable biocompatibility, biodegradability, and osteoconductivity properties (13). These are non-toxic polymers widely used as biomaterials in this regard. Therefore, the purpose of the current research was to develop a drug delivery system based on coated IONPs to enhance the therapeutic efficacy of curcumin. We evaluated the physicochemical properties of the nanoparticles (NPs) and determined the drug release profile. The anti-cancer effects of the nanoformulations were assessed against the HT-29 and MCF-7 cell lines, representing colon and breast cancers, respectively.

2. Objectives

The main purpose of this study was to evaluate and compare the cytotoxic effects of curcumin-loaded IONPs and free curcumin against the HT-29 (colon) and MCF-7 (breast) cancer cell lines.

3. Methods

3.1. Materials

Curcumin, calcium nitrate tetra hydrate $\text{Ca}(\text{NO}_3)_2 \cdot 4\text{H}_2\text{O}$, diammonium hydrogen phosphate $(\text{NH}_4)_2\text{HPO}_4$, iron (III) chloride (FeCl_3), ferrous sulphate heptahydrate ($\text{FeSO}_4 \cdot 7\text{H}_2\text{O}$), MTT reagent, and TWEEN® 80 were purchased from Sigma-Aldrich (USA). Ethanol (EtOH , $\geq 99.8\%$, HPLC), methanol anhydrous (MeOH , 99.8%), alginic acid sodium salt (NaAlg, low viscosity), and dimethylsulfoxide (DMSO) were purchased from Merck (Germany). The HT-29 and MCF-7 cancer cell lines were purchased from Pastor Institute Cell bank (Iran, Tehran).

3.2. Synthesis of HAP- and NaAlg-coated IONPs

Iron oxide nanoparticles were synthesized by the coprecipitation technique. Briefly, 3.2 g FeCl_3 and 2.78 g FeSO_4 were dissolved in distilled water, and NaOH solution was then added to the solution. A 20-minute degassing was performed under nitrogen atmosphere. The resulting precipitate was collected magnetically, washed with deionized

water several times, and then dried. The obtained product was used for HAp and NaAlg coating. Then 0.5 g of IONPs was dissolved in distilled water and mixed with NaAlg powder and 0.25 M $\text{Ca}(\text{NO}_3)_2$ and $(\text{NH}_4)_2\text{HPO}_4$. The pH of the system was maintained in the range of 8-9. Finally, the resultant was washed 2-3 times with deionized water (12).

3.3. In Vitro Loading of Curcumin into IONPs

For the loading of curcumin into IONPs coated with HAP-NaAlg, 5 mg of curcumin was dissolved in acetone and added dropwise to 20 mg of an IONP/HAP-NaAlg aqueous suspension, followed by stirring at 400 rpm for 24 h to allow curcumin to permeate into the NPs. At the end, the resulting mixture was washed to separate free curcumin from the coated IONPs containing curcumin (14).

3.4. Drug Loading and Encapsulation Efficiency

Free curcumin level was determined in the supernatant obtained after the production of the NPs. To evaluate drug loading (DL) efficiency, the NPs were centrifuged at 11,000 rpm and 4°C for 30 minutes, and the resulting suspension was used for calculating DL amount. Also, the amount of free curcumin was determined by UV-Vis spectrophotometry at 450 nm (14). The measurement was repeated three times. Encapsulation efficiency (EE) and DL were calculated as follows:

$$EE (\%) = \frac{[Total\ Curcumin] - [Free\ Curcumin]}{[Total\ Curcumin]} \times 100 \quad (1)$$

$$DL (\%) = \frac{[Total\ Curcumin] - [Free\ Curcumin]}{[IONPs]} \times 100 \quad (2)$$

3.5. Scanning Electron Microscopy

To evaluate surface morphology, scanning electron microscopy (SEM) (Philips XL30, the Netherlands) was used.

3.6. Transmission Electron Microscopy

To evaluate the size of IONPs, transmission electron microscopy (TEM) (JEOL, Tokyo, Japan) was used. A drop of IONP suspension was placed on a carbon coated copper TEM grid and allowed to air-dry. The dried samples were then examined at 120 kV under the microscope.

3.7. Fourier Transform Infrared Spectroscopy

For Fourier transform infrared (FTIR) spectroscopy analysis, IONPs, NaAlg/HAP, IONPs@NaAlg/HAP, curcumin, and IONPs@NaAlg/HAP-curcumin were scanned over a wave range of 4000 - 400 cm^{-1} using an FTIR spectrophotometer (Perkin Elmer 65, USA) to determine possible chemical bonds between the drug and NPs.

3.8. X-ray Diffraction Study

To determine the crystalline structure of the IONPs, X-ray diffraction (XRD) patterns were measured. The experiment was performed by a D/Max-B Rikagu diffractometer (AW-XDM300, the UK). All the experiments were performed at room temperature.

3.9. In Vitro Drug Release

To measure the in vitro release of curcumin from IONPs, 3 mg of the sample was transferred into 6 mL of PBS (pH = 7.5 or 5.5) containing 0.1% w/v Tween-80 and stirred at 100 rpm and 37°C. At certain time points, 1 mL of the solution was replaced with the same amount of fresh PBS. The mixture was then centrifuged (8000 rpm, 25 min). The absorbance of each sample was measured by an UV-Visible spectrophotometer at 450 nm, and the concentration of curcumin released from IONPs was determined using a standard calibration curve (14).

3.10. In Vitro Cytotoxicity Assessment

The cytotoxic effects of coated IONPs, free curcumin, and curcumin-loaded IONPs were assessed against the HT-29 and MCF-7 cancer cell lines by the MTT assay. Briefly, cells were plated at a density of 1×10^4 cells per well in 96-well plates and cultivated at 37°C in humidified air containing 5% CO₂ (Heal Force HF-90, Japan) for 24 h. Then the cells were treated with various concentrations (20 - 80 µg/mL) of coated IONPs, free curcumin, and curcumin-loaded IONPs and incubated for 24, 48, and 72 h at 37°C (14). After the specified incubation time, the culture medium was discarded, and 20 µL of MTT (5 mg/mL) solution was added to each well, and incubation continued for 4 h at 37°C. The supernatant was withdrawn, and 150 µL DMSO was added to each well to dissolve formazan crystals. The UV absorption of soluble formazan crystals was determined using spectrophotometry at 570 nm by a microplate reader. The experiment was performed in triplicate (15). The viability of the cells was calculated using the following equation:

$$\text{Cell viability \%} = \frac{\text{Abs}_{\text{test cells}}}{\text{Abs}_{\text{control cells}}} \times 100 \quad (3)$$

Where $\text{Abs}_{\text{test cells}}$ and $\text{Abs}_{\text{control cells}}$ are the amount of formazan in treated and non-treated cells, respectively.

3.11. Flow Cytometry

For apoptosis assessment, HT-29 and MCF-7 cells were treated for 72 hours. After washing with PBS and trypsin, the cells were separated from the culture medium by centrifugation. The cells were washed with the buffer solution

and centrifuged at 15,000 rpm for 15 minutes. After that, 5 µL of annexin-V (BD Pharmingen) and Propidium iodide were added to the cells, and the cells were incubated for 15 minutes at room temperature in dark and then evaluated by flow cytometry (BD FACS Calibur) (16).

3.12. Statistical Analysis

All results were expressed as mean \pm SD. Statistical analysis was conducted by one-way ANOVA, and p values less than 0.05 were considered statistically significant.

4. Results

4.1. IONPs' Characterization

4.1.1. Assessment of DL Efficiency

Drug encapsulation efficiency is an important factor to investigate the performance of drug carriers. Curcumin-encapsulated IONPs were prepared 21.03 ± 0.87 drug loaded in the nanoparticles and showed $84.16 \pm 3.51\%$ encapsulation efficiency.

4.1.2. SEM and TEM Analyses

The results of SEM showed that the prepared NPs were spherical in shape and relatively monodisperse in size (Figure 1A). Also, TEM results showed spherical and smooth surfaces in NPs with an average particle size of 5 - 7 nm. (Figure 1B). No aggregation or adhesion was observed in microscopic images. Although the particles seemed to be agglomerated in electron microscopy analysis, this was probably due to the dry state of the NPs, which could be easily resolved in water to obtain separate particles or less accumulation.

4.1.3. FTIR Analysis

The FTIR spectra of NaAlg/HAP, IONPs@NaAlg/HAP, curcumin, and IONPs@NaAlg/HAP-curcumin after absorption have been shown in Figure 2. The FTIR spectrum of the IONPs showed significant absorption bands around 630 and 3423 cm⁻¹, which are related to the tensile vibration of the Fe-O and O-H groups of IONPs. In the FTIR spectrum of HAP-NaAlg nanoparticles, the absorption peaks around 570, 1046, 1384, 1637, and 3426 cm⁻¹ were related to the stretching modes of the O-H group (17). The FTIR spectrum of IONPs@HAP/NaAlg particles showed the apparent interactions of sodium alginate with both hydroxyapatite and IONPs, characterized by COOH symmetrical and asymmetrical tensile vibrations at 1625 cm⁻¹ and 1384 cm⁻¹, respectively (18, 19). As shown, the spectrum of IONPs had three absorption peaks around 583, 1627, and 3423 cm⁻¹,

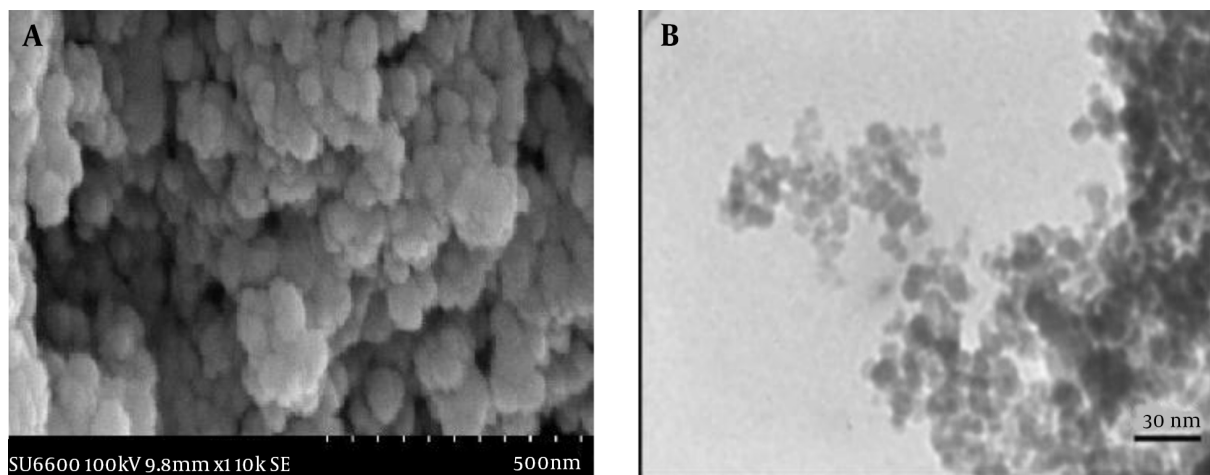


Figure 1. A, SEM images and B, TEM images of iron oxide nanoparticles.

with the highest absorption intensity at 583 cm^{-1} . The diagrams of the hydroxyapatite and sodium alginate coatings also showed absorption peaks around $823, 562, 1046, 1384, 1637, 3426, 2005,$ and 3426 cm^{-1} , with the latest two showing the highest absorption. The spectrum of the IONPs coated with hydroxyapatite, and sodium alginate demonstrated absorption peaks at $563, 1030, 1625, 2005, 2923,$ and 3424 cm^{-1} , with more intensity at the wave numbers of $563, 1030,$ and 3424 cm^{-1} . Strong absorption around 563 cm^{-1} was due to the crystal structure of iron oxide. On the other hand, a significant absorption at 3424 cm^{-1} resulted from the overlap of 3423 cm^{-1} (related to pure IONPs) and 3426 cm^{-1} (related to hydroxyapatite and sodium alginate) absorption peaks. Other absorption peaks observed in the spectrum of the IONPs coated with hydroxyapatite and sodium alginate, such as 1030 cm^{-1} and 2005 cm^{-1} , are very similar to those of hydroxyapatite and sodium alginate, all of which indicated the success of the coating process. The correct coating of hydroxyapatite and sodium alginate depends on the iron nano oxide sample. Similarly, the main absorption peaks around $1200, 1400, 1600, 2800,$ and 3400 cm^{-1} were in fact due to overlapping peaks. These main absorption peaks corresponded to the iron oxide sample coated with hydroxyapatite and sodium alginate, which were both loaded with curcumin. The absorption peaks indicated that the NPs were successfully coated and then loaded with curcumin.

4.1.4. XRD Analysis

The XRD patterns of the IONPs have been depicted in [Figure 3](#), the XRD pattern at 2θ of $30.1, 35.6, 43.3, 53.5, 57.63,$ and 74 demonstrated that the synthesized magnetic NPs

had a crystal structure. The XRD pattern confirmed the crystallography and different phases of the studied NP formulations ([20](#)).

4.1.5. In Vitro Drug Release

[Figure 4](#) represents curcumin release pattern from coated IONPs at two different pH (5.5 and 7.5). The results demonstrated an abrupt release during the first 20 to 24 hours at both pH, which then continued steadily for 240 hours. However, the amount of released curcumin was higher at pH 5.5 , followed by a more gradual release at longer periods of time until reaching a release percentage of $96.77 \pm 0.68\%$ while this rate was about $44.24 \pm 0.59\%$ at pH 7.5 . This may be explained by the slow degradation of HAp-coated materials in acidic media. Since cancerous cells have a pH lower than that of normal cells, this faster release at the lower pH can enhance the effectiveness of targeting tumors and drug release into tumor microenvironment ([21](#)).

4.1.6. In Vitro Cytotoxicity

The in vitro cytotoxic effects of HAP/NaAlg-coated IONPs, free curcumin, and curcumin-loaded IONPs were assessed against the HT-29 and MCF-7 cancer cell lines by the MTT test after 24, 48, and 72 h of treatment. No obvious cytotoxicity was observed for the IONPs coated with HAP/NaAlg at the studied concentrations. Both free curcumin and curcumin-loaded IONPs exhibited concentration- and time-dependent cytotoxicity. The anti-proliferative effect of curcumin-loaded IONPs was significantly higher than that of free curcumin at the

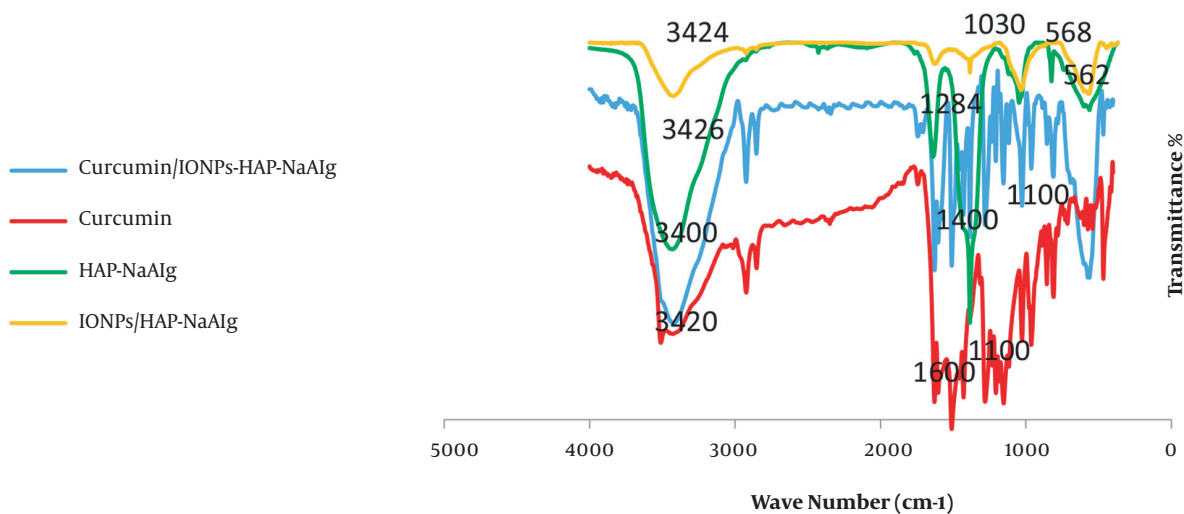


Figure 2. Comparison of the FTIR spectra of HAP and NaAlg (green), IONPs/HAP-NaAlg (yellow), curcumin (red), and IONPs/HAP-NaAlg/curcumin (blue).

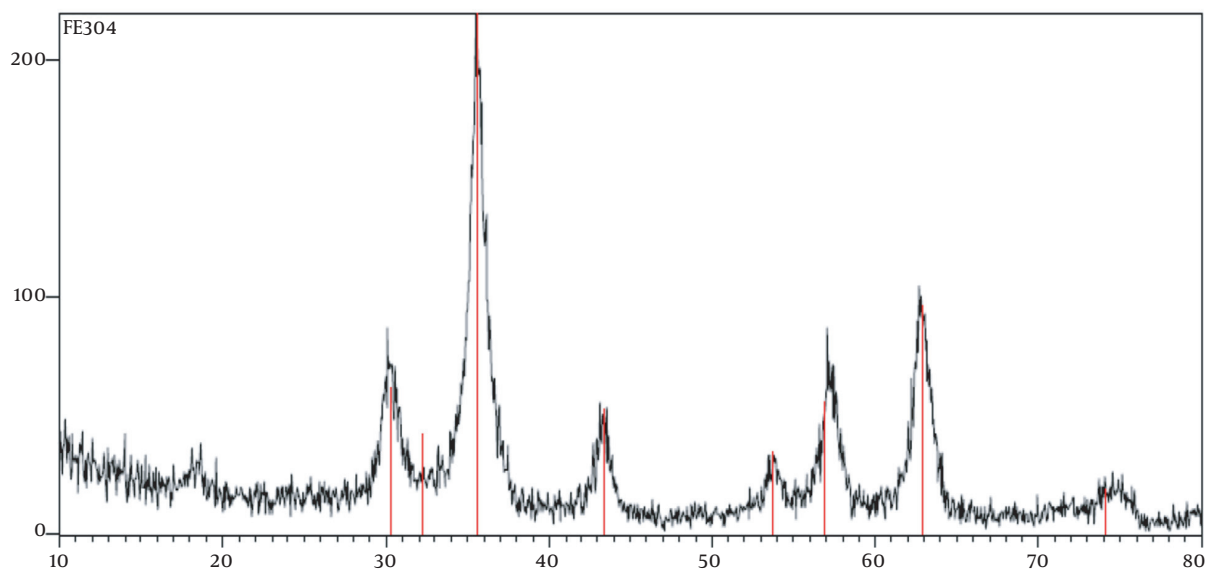


Figure 3. The X-ray diffraction pattern of IONPs.

same concentration and incubation time (Figures 5 and 6).

The results showed that at 24, 48, and 72 hours after treating the cell lines with curcumin-loaded IONPs, the mean percentage of cell survival at all concentrations was significantly different compared with the control group ($P < 0.001$).

Higher IC_{50} values (Tables 1 and 2), as the drug concentration required to inhibit the growth of 50% of tu-

mor cells (HT-29 and MCF-7) during a certain period, were obtained for free curcumin and curcumin-loaded coated IONPs, confirming the higher cytotoxic effects of curcumin-loaded IONPs.

4.1.7. Flow Cytometry

The results of annexin/PI staining to determine alive/apoptotic/late apoptotic/dead HT-29 and MCF-7 cells have been presented in Figures 7 and 8, respectively. The

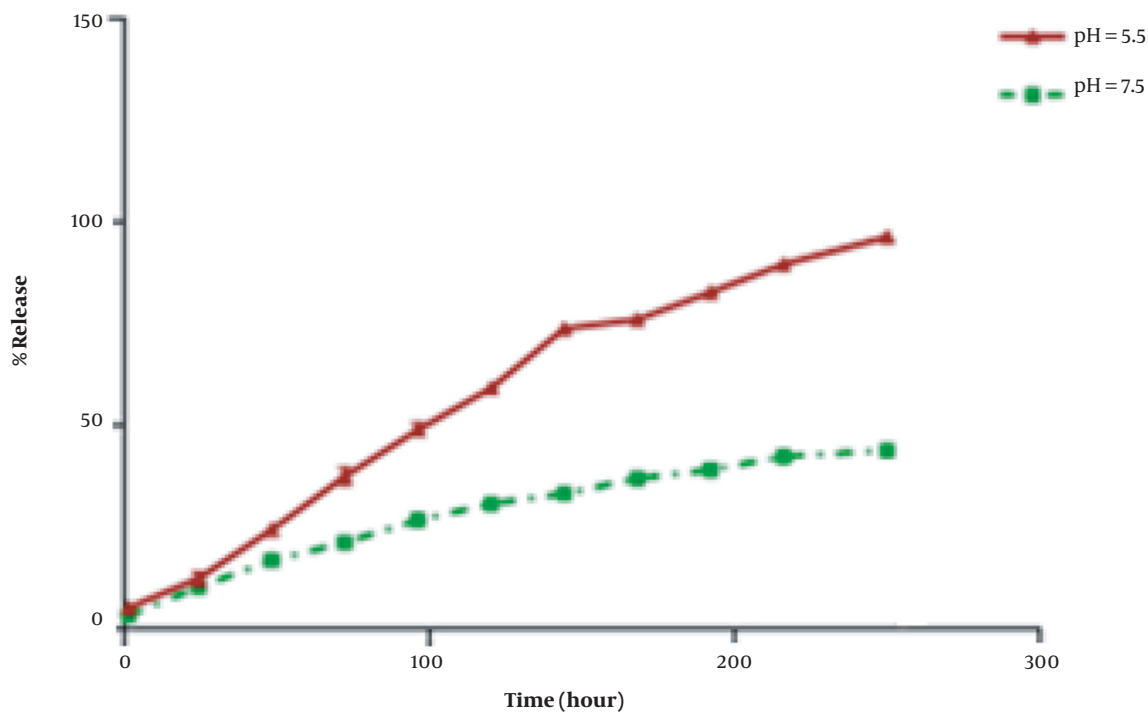


Figure 4. In vitro cumulative release percentage of curcumin% from IONPs/HAP-NaAlg under two buffer conditions (pH = 5.5 and 7.5).

Table 1. The IC₅₀ Values of Free Curcumin and Curcumin-Loaded Coated IONPs Against the HT-29 Cell Line After 24, 48, and 72 h of Incubation (N = 3)^a

IC ₅₀ (μg/mL) HT-29 Cell Line		
Time, h	Curcumin	Curcumin-Loaded Coated IONPs
24	1.18 ± 120.23	1.15 ± 79.04
48	1.15 ± 86.04	1.15 ± 57.62
72	1.13 ± 62.66	1.12 ± 42.14

^aValues are expressed as mean ± SD.

Table 2. The IC₅₀ Values of Free Curcumin and Curcumin-Loaded Coated IONPs Against the MCF-7 Cell Line After 24, 48, and 72 h of Incubation (N = 3)^a

IC ₅₀ (μg/mL) MCF-7 Cell Line		
Time, h	Curcumin	Curcumin Loaded Coated IONPs
24	1.17 ± 136.14	1.13 ± 103.97
48	1.15 ± 98.93	1.14 ± 70.29
72	1.13 ± 67.16	1.12 ± 46.86

^aValues are expressed as mean ± SD.

results showed that in comparison with free curcumin, the cells treated with curcumin-loaded HAp/NaAlg-coated IONPs showed a higher percentage of cells in either the

late-apoptosis, necrosis, or death phases.

Regarding the HT-29 cell line, the percentage of alive cells in the control group was 87.4%, which was higher than that of other groups. The percentage of apoptotic cells increased from 9.20% in the cells incubated with curcumin to 44.1% in those incubated with curcumin-loaded HAp/NaAlg-coated IONPs. Moreover, the percentage of cells in late apoptosis rose from 6.82% in the cells incubated with curcumin to 11.2% in the cells incubated with curcumin-loaded HAp/NaAlg-coated IONPs.

For MCF-7 cells, the percentage of alive cells in the control group was 78.3%, which was higher compared to other groups. The percentage of apoptotic cells increased from 1.22% in the cells incubated with curcumin to 12.9% in those incubated with curcumin-loaded HAp/NaAlg-coated IONPs. Moreover, the percentage of cells in late apoptosis rose from 10.8% in the cells incubated with curcumin to 20.3% in the cells incubated with curcumin-loaded IONPs-HAp-NaAlg.

5. Discussion

The significant cytotoxic activity of curcumin against various human cancer cells has been reported in the liter-

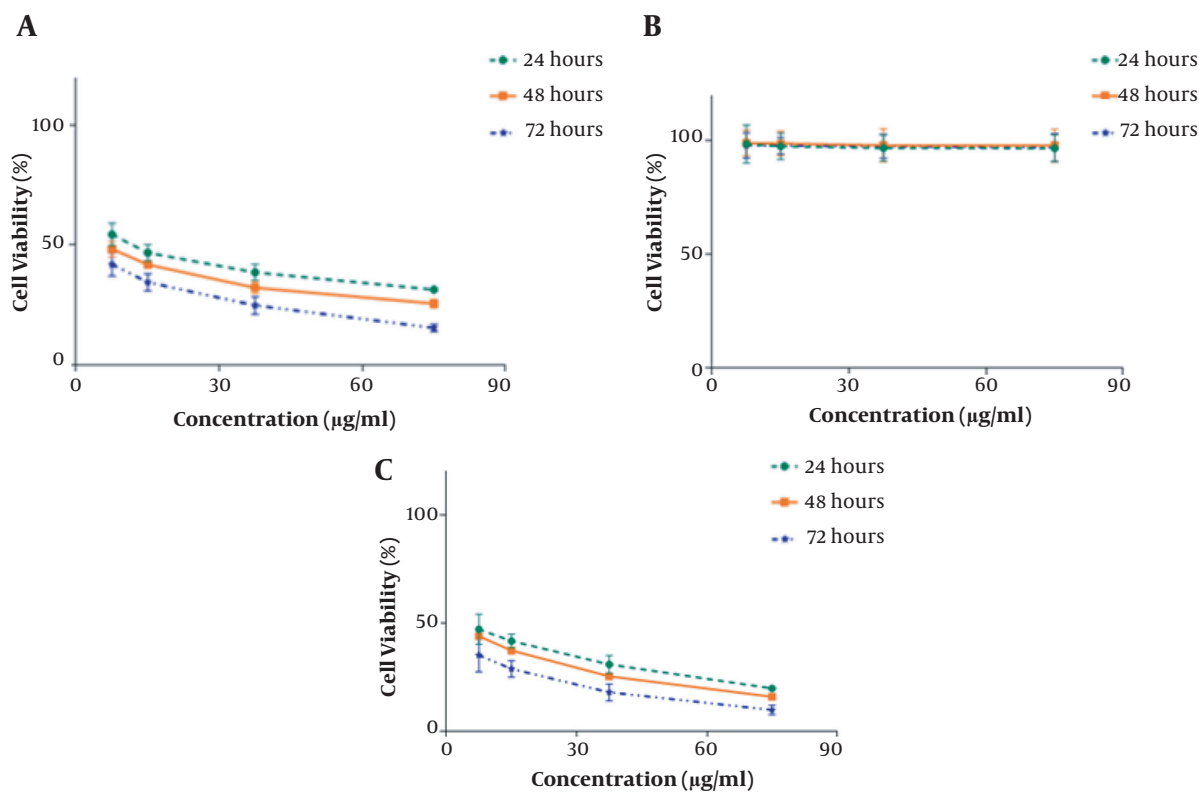


Figure 5. Viability of the HT-29 cells treated with 20, 40, 60, and 80 µg/mL of (A) curcumin, (B) coated IONPs, and (C) curcumin-loaded coated IONPs for 24, 48, and 72 h (mean \pm SD, P-value < 0.001).

ature. Curcumin exerts its anti-cancer activity in various ways and by interfering with intracellular signaling pathways. Curcumin can induce or inhibit the production of a variety of cytokines and enzymes, such as MAPK, NF κ B, COX-2, and I κ B β (22). Nevertheless, curcumin is extremely hydrophobic, which is a major obstacle to its successful application as a therapeutic agent.

In order to resolve this limitation, structural modifications and targeted drug delivery systems can be used. Iron oxide nanoparticles can deliver various anti-cancer compounds, such as chemotherapeutics, peptides, and active compounds, to tumor cells in a dose-dependent manner, reducing drug-induced toxicity towards healthy cells. These nanoparticles have been utilized to suppress the growth of tumor cells.

This study was carried out to improve curcumin bioavailability without influencing its biological properties, by loading it into IONPs, which were successfully prepared by the co-precipitation technique. Particle size is considered an important factor in determining the efficacy of drug delivery systems because it affects the phar-

maceutical properties of the drug, including its release profile and cellular uptake. In this study, the high drug loading and entrapment efficiency ensured the successful preparation of curcumin-loaded IONPs, suggesting a strong interaction between curcumin, as a hydrophobic drug, and hydroxyapatite-coated IONPs (18). The FTIR analysis revealed no chemical interaction between IONPs and curcumin, ensuring that curcumin could be entrapped into the NPs without alteration in its natural structure. The XRD pattern confirmed the crystalline nature of the synthesized IONPs. The maximum release rate of curcumin was observed at pH = 5.5, suggesting that the release process could be facilitated by the slow degradation of HAp-coating materials in acidic media (20, 23). Since cancerous cells have pH lower than normal cells, this faster release at the lower pH can be beneficial for targeting tumors because of their acidic microenvironments.

The therapeutic efficacy of a drug strongly depends on its concentration and duration of availability at the tumor site. In the present study, the sustained release observed indicated that the coated IONPs could be suitable carriers

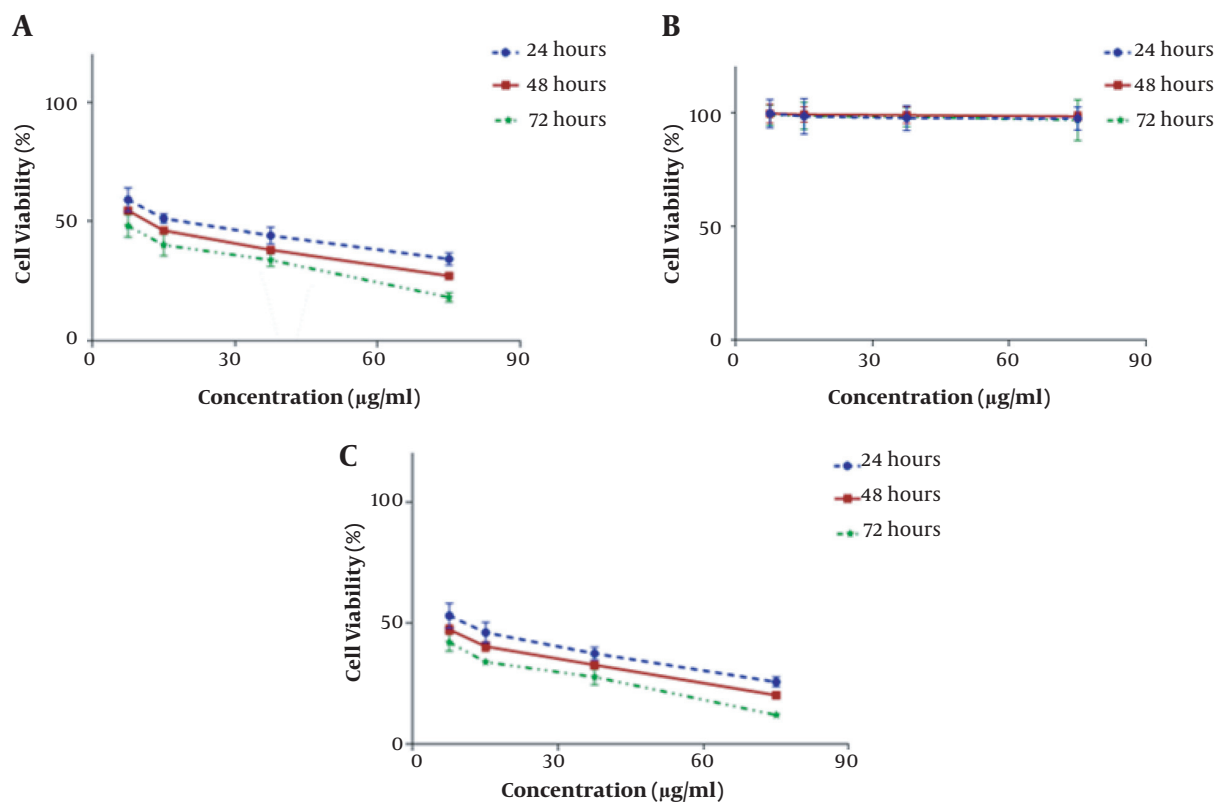


Figure 6. Viability of the MCF-7 cells treated with 20, 40, 60, and 80 µg/ml of A, Curcumin; B, Coated IONPs; and C, Curcumin-loaded coated IONPs for 24, 48, and 72 h (mean \pm SD, P-value < 0.001).

for targeting tumors by allowing sustained and prolonged release of curcumin, boosting its therapeutic effects (8). Our results demonstrated that IONPs alone had no cytotoxic effects, ensuring their biosafety and non-toxic nature. The relatively low IC_{50} values of curcumin-loaded coated IONPs against the evaluated cancer cell lines are probably due to the small size of the NPs and the controlled release of curcumin from the nano-carriers compared to the rapid release of neat drugs. Our results showed that after 24, 48, and 72 hours of treating the cell lines with curcumin-loaded coated IONPs, the mean percentage of cell survival at all concentrations was significantly different from that of the control group ($P < 0.001$). Consistent with the results of this study, Thu et al. (8) showed the higher efficacy of $Fe_3O_4/OCMCs/Cur$ against the HT-29 cancer cell line (8). In vivo studies on Balb/c mice showed a considerable decline in tumor development and increased survival in tumor-bearing mice treated with cisplatin-loaded IONPs (24).

Preclinical and clinical studies on IONPs have demonstrated a complex interaction between these NPs and the immune system, depending on the properties of the NPs

and the type and condition of the host. Iron oxide nanoparticles have had a variety of useful primary applications; however, for being used in clinical settings, there is a need for more studies on animal models and evaluating preclinical results (25). Our results indicated that the curcumin-loaded IONPs had a considerably higher ability to induce apoptosis in cancerous cells compared to free curcumin, probably due to the higher uptake of the drug-loaded NPs (26).

5.1. Conclusions

Nanotechnology in the field of pharmaceuticals seeks new models for targeted drug delivery to tumor cells, which is more effective in suppressing cancer progression and reducing drug side effects. Therefore, it is essential to find anti-tumor compounds that have fewer side effects, and herbal medicines are among these compounds.

In the present study, IONPs were synthesized, coated with HAp/NaAlg, and then loaded with curcumin. Curcumin release was measured for 10 days, which showed

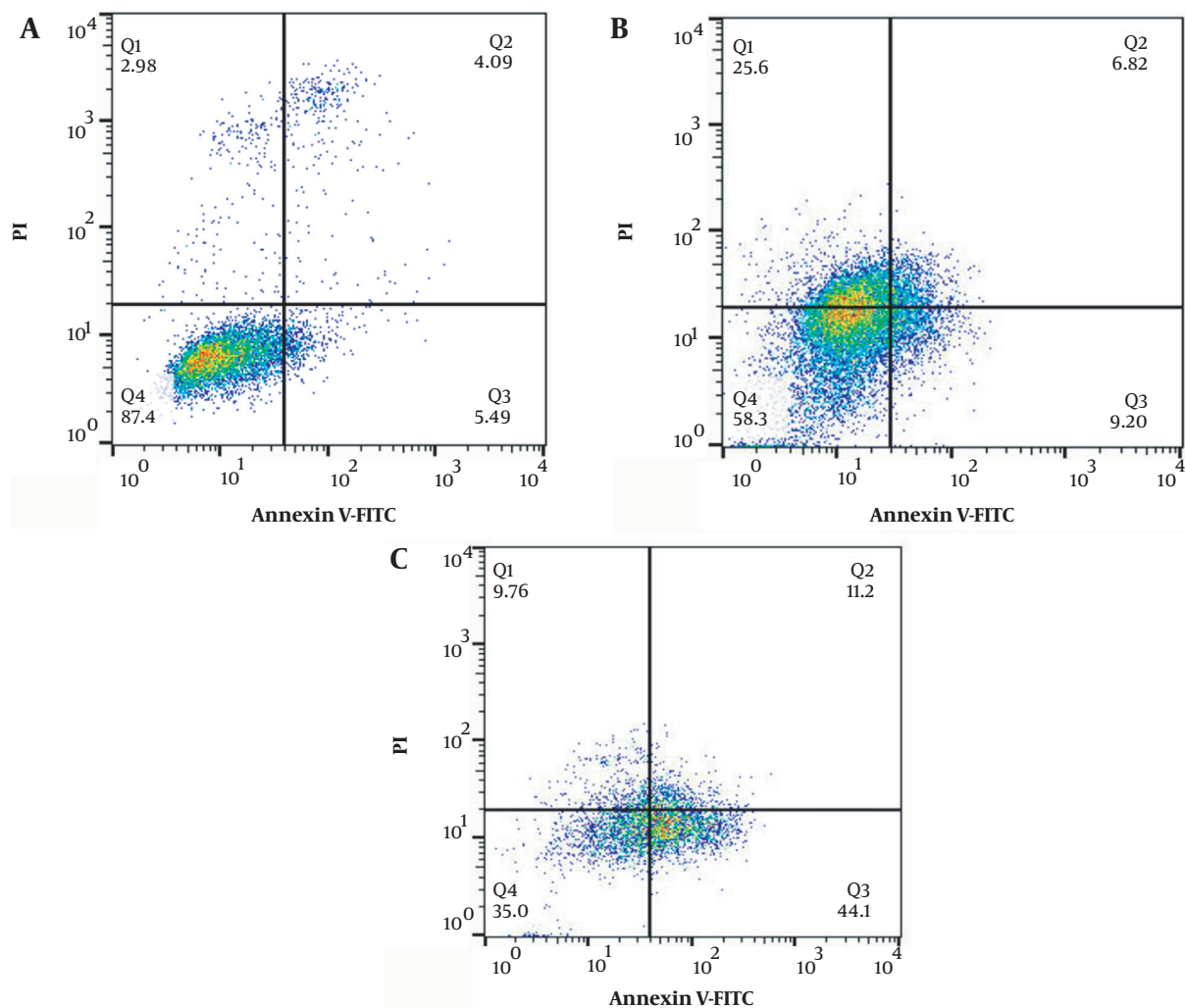


Figure 7. Flow cytometric analysis of HT-29 cells. A, Control group; B, Curcumin; and C, Curcumin-loaded coated IONPs.

a faster release in acidic pH (i.e., mimicking tumor microenvironment). Anti-proliferative tests showed that IONPs@HAP-NaAlg@Curcumin had high cytotoxicity against colon and breast cancer cells, with IC₅₀ values lower than that of free curcumin. Flow cytometry results also confirmed the results of the MTT assay, indicating that curcumin-coated IONPs increased the rate of apoptosis in the cancer cell lines.

Curcumin-coated IONPs showed good cytotoxic effects against both HT-29 and MCF-7 cells, and this effect was more prominent against HT-29 cells. Therefore, this formulation can be regarded as an anti-tumor compound for treating various cancers, including colon and breast cancers. Before conducting clinical trials in humans, experimental studies should be performed on large rodents.

Acknowledgments

The authors are grateful to the Islamic Azad University, Falavarjan branch for its cooperation and providing necessary facilities.

Footnotes

Authors' Contribution: Kahin Shahanipour developed the main idea and conducted the research. Soheil Fatahian and Masoomeh Nobahari contributed in chemical experiments for the preparation and characterization of nanoparticles. Ramesh Monajemi and Masoomeh Nobahari performed cell culture experiments and statistical analysis. Kahin Shahanipour and Masoomeh Nobahari

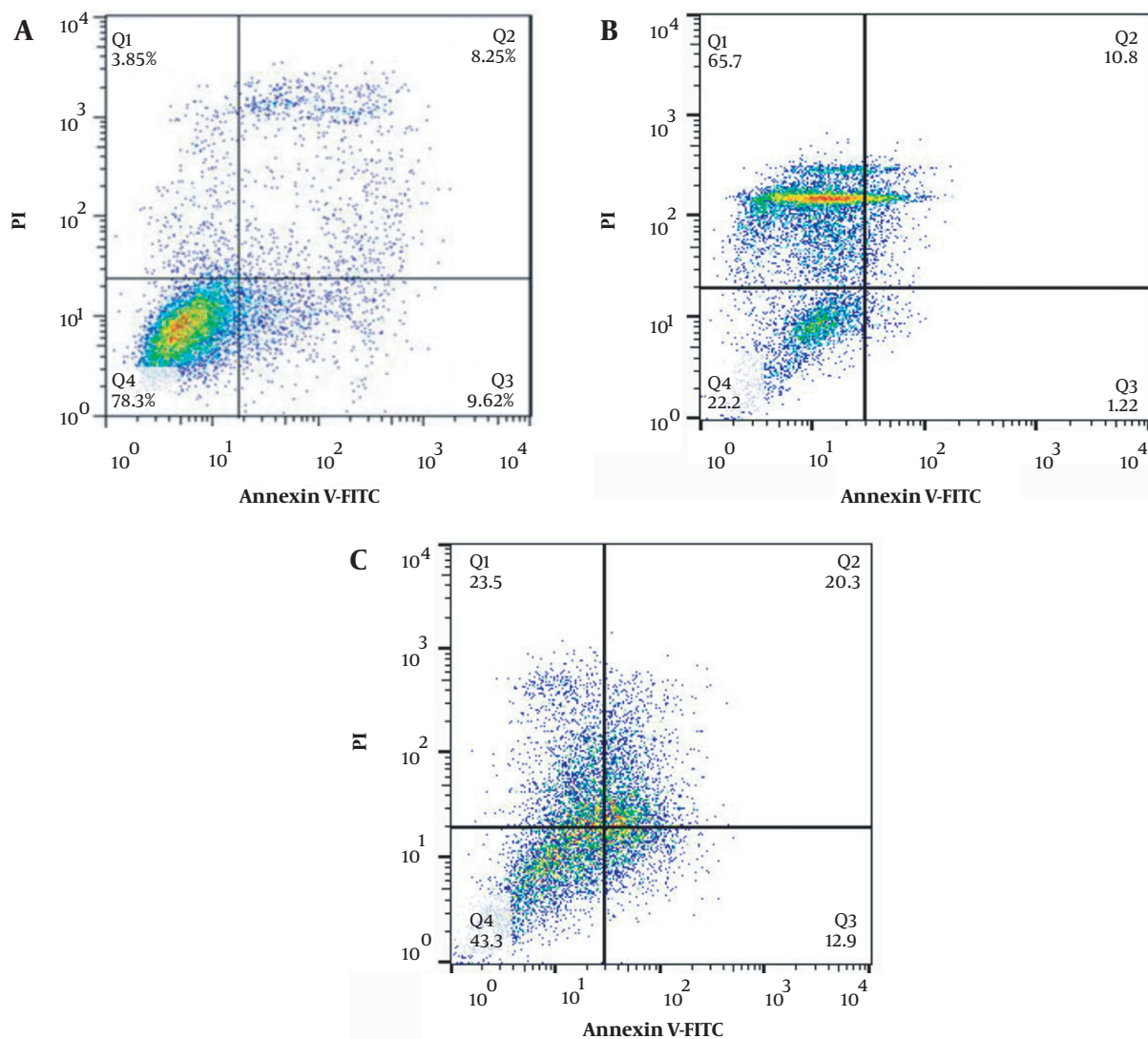


Figure 8. Flow cytometric analysis of MCF-7 cells. A, Control group; B, Curcumin; and C, curcumin-loaded coated IONPs.

wrote and submitted the manuscript. All authors read and approved the final version of the manuscript.

Conflict of Interests: The authors declare no conflict of interest.

Ethical Approval: Ethical issues, including plagiarism, falsification, misconduct, data fabrication, double publication, or redundancy, were carefully observed. The ethical committee of Islamic Azad University of Falavarjan approved the protocol (ethical code: IR.IAU.FALA.REC.1397.001).

Funding/Support: None.

References

1. Radhakrishnan EK, Bava SV, Narayanan SS, Nath LR, Thulasidasan AK, Soniya EV, et al. [6]-Gingerol induces caspase-dependent apoptosis and prevents PMA-induced proliferation in colon cancer cells by inhibiting MAPK/AP-1 signaling. *PLoS One*. 2014;9(8): e104401. doi: [10.1371/journal.pone.0104401](https://doi.org/10.1371/journal.pone.0104401). [PubMed: 25157570]. [PubMed Central: PMC4144808].
2. Wang Y, Yu J, Cui R, Lin J, Ding X. Curcumin in Treating Breast Cancer: A Review. *J Lab Autom*. 2016;21(6):723-31. doi: [10.1177/2211068216655524](https://doi.org/10.1177/2211068216655524). [PubMed: 27325106].
3. Anjum F, Razvi N, Masood M. Breast Cancer Therapy: A Mini Review. *MOJ Drug Design Develop Ther*. 2017;1(2). doi: [10.15406/mojddt.2017.01.00006](https://doi.org/10.15406/mojddt.2017.01.00006).

4. Abdel-Moneim A, Magdy A. Review on Medicinal Plants as Potential Sources of Cancer Prevention and Treatment. *Eur J Biomed*. 2016;**3**(6):45-62.
5. Khan T, Ali M, Khan A, Nisar P, Jan SA, Afridi S, et al. Anticancer Plants: A Review of the Active Phytochemicals, Applications in Animal Models, and Regulatory Aspects. *Biomolecules*. 2019;**10**(1). doi: [10.3390/biom10010047](https://doi.org/10.3390/biom10010047). [PubMed: [31892257](https://pubmed.ncbi.nlm.nih.gov/31892257/)]. [PubMed Central: [PMC7022400](https://pubmed.ncbi.nlm.nih.gov/PMC7022400/)].
6. Poonam S, Chandana M. A Review on Anticancer Natural Drugs. *Int J PharmTech Res*. 2015;**8**(7):131-41.
7. Alizadeh AM, Khaniki M, Azizian S, Mohaghheghi MA, Sadeghizadeh M, Najafi F. Chemoprevention of azoxymethane-initiated colon cancer in rat by using a novel polymeric nanocarrier-curcumin. *Eur J Pharmacol*. 2012;**689**(1-3):226-32. doi: [10.1016/j.ejphar.2012.06.016](https://doi.org/10.1016/j.ejphar.2012.06.016). [PubMed: [22709992](https://pubmed.ncbi.nlm.nih.gov/22709992/)].
8. Thu HP, Huong LTT, Nhung HTM, Tham NT, Tu ND, Thi HTM, et al. Fe₃O₄/o-Carboxymethyl Chitosan/Curcumin-based Nanodrug System for Chemotherapy and Fluorescence Imaging in HT29 Cancer Cell Line. *Chem Let*. 2011;**40**(11):1264-6. doi: [10.1246/cl.2011.1264](https://doi.org/10.1246/cl.2011.1264).
9. Hosseinimehr SJ. A review of preventive and therapeutic effects of curcumin in patients with cancer. *J Clin Excellence*. 2014;**2**(2):50-63.
10. Vilar G, Tulla-Puche J, Albericio F. Polymers and drug delivery systems. *Curr Drug Deliv*. 2012;**9**(4):367-94. doi: [10.2174/156720112801323053](https://doi.org/10.2174/156720112801323053). [PubMed: [22640038](https://pubmed.ncbi.nlm.nih.gov/22640038/)].
11. Rosen JE, Chan L, Shieh DB, Gu FX. Iron oxide nanoparticles for targeted cancer imaging and diagnostics. *Nanomedicine*. 2012;**8**(3):275-90. doi: [10.1016/j.nano.2011.08.017](https://doi.org/10.1016/j.nano.2011.08.017). [PubMed: [21930108](https://pubmed.ncbi.nlm.nih.gov/21930108/)].
12. Manatunga DC, de Silva RM, de Silva KMN, de Silva N, Bhandari S, Yap YK, et al. pH responsive controlled release of anti-cancer hydrophobic drugs from sodium alginate and hydroxyapatite bi-coated iron oxide nanoparticles. *Eur J Pharm Biopharm*. 2017;**117**:29-38. doi: [10.1016/j.ejpb.2017.03.014](https://doi.org/10.1016/j.ejpb.2017.03.014). [PubMed: [28330763](https://pubmed.ncbi.nlm.nih.gov/28330763/)].
13. Salehi M, Ai A, Ehterami A, Einabadi M, Taslimi A, Ai A, et al. In vitro and In vivo Investigation of poly (lactic acid)/hydroxyapatite nanoparticle scaffold containing nandrolone decanoate for the regeneration of critical-sized bone defects. *Nanomed J*. 2020;**7**(2):115-23.
14. Akrami M, Khoobi M, Khalilvand-Sedagheh M, Haririan I, Bahador A, Faramarzi MA, et al. Evaluation of multilayer coated magnetic nanoparticles as biocompatible curcumin delivery platforms for breast cancer treatment. *RSC Adv*. 2015;**5**(107):88096-107. doi: [10.1039/c5ra13838h](https://doi.org/10.1039/c5ra13838h).
15. Zeng L, Yan J, Luo L, Ma M, Zhu H. Preparation and characterization of (-)-Epigallocatechin-3-gallate (EGCG)-loaded nanoparticles and their inhibitory effects on Human breast cancer MCF-7 cells. *Sci Rep*. 2017;**7**:45521. doi: [10.1038/srep45521](https://doi.org/10.1038/srep45521). [PubMed: [28349962](https://pubmed.ncbi.nlm.nih.gov/28349962/)]. [PubMed Central: [PMC5368574](https://pubmed.ncbi.nlm.nih.gov/PMC5368574/)].
16. Manatunga DC, de Silva RM, de Silva KMN, Malavige GN, Wijeratne DT, Williams GR, et al. Effective delivery of hydrophobic drugs to breast and liver cancer cells using a hybrid inorganic nanocarrier: A detailed investigation using cytotoxicity assays, fluorescence imaging and flow cytometry. *Eur J Pharm Biopharm*. 2018;**128**:18-26. doi: [10.1016/j.ejpb.2018.04.001](https://doi.org/10.1016/j.ejpb.2018.04.001). [PubMed: [29625162](https://pubmed.ncbi.nlm.nih.gov/29625162/)].
17. Jegan A, Ramasubbu A, Saravanan S, Vasanthkumar S. One-pot synthesis and characterization of biopolymer-iron oxide nanocomposite. *Int J Nano Dimens*. 2011;**2**(2):105-10.
18. Liao SH, Liu CH, Bastakoti BP, Suzuki N, Chang Y, Yamauchi Y, et al. Functionalized magnetic iron oxide/alginate core-shell nanoparticles for targeting hyperthermia. *Int J Nanomedicine*. 2015;**10**:3315-27. doi: [10.2147/IJN.S68719](https://doi.org/10.2147/IJN.S68719). [PubMed: [26005343](https://pubmed.ncbi.nlm.nih.gov/26005343/)]. [PubMed Central: [PMC4427608](https://pubmed.ncbi.nlm.nih.gov/PMC4427608/)].
19. Painter PC, Snyder RW, Starsinic M, Coleman MM, Kuehn DW, Davis A. Concerning the Application of FT-IR to the Study of Coal: A Critical Assessment of Band Assignments and the Application of Spectral Analysis Programs. *Appl Spectrosc*. 2016;**35**(5):475-85. doi: [10.1366/0003702814732256](https://doi.org/10.1366/0003702814732256).
20. Cai H, An X, Cui J, Li J, Wen S, Li K, et al. Facile hydrothermal synthesis and surface functionalization of polyethyleneimine-coated iron oxide nanoparticles for biomedical applications. *ACS Appl Mater Interfaces*. 2013;**5**(5):1722-31. doi: [10.1021/am302883m](https://doi.org/10.1021/am302883m). [PubMed: [23388099](https://pubmed.ncbi.nlm.nih.gov/23388099/)].
21. Bano S, Afzal M, Waraich MM, Alamgir K, Nazir S. Paclitaxel loaded magnetic nanocomposites with folate modified chitosan/carboxymethyl surface; a vehicle for imaging and targeted drug delivery. *Int J Pharm*. 2016;**513**(1-2):554-63. doi: [10.1016/j.ijpharm.2016.09.051](https://doi.org/10.1016/j.ijpharm.2016.09.051). [PubMed: [27651326](https://pubmed.ncbi.nlm.nih.gov/27651326/)].
22. Tomeh MA, Hadianamrei R, Zhao X. A Review of Curcumin and Its Derivatives as Anticancer Agents. *Int J Mol Sci*. 2019;**20**(5). doi: [10.3390/ijms20051033](https://doi.org/10.3390/ijms20051033). [PubMed: [30818786](https://pubmed.ncbi.nlm.nih.gov/30818786/)]. [PubMed Central: [PMC6429287](https://pubmed.ncbi.nlm.nih.gov/PMC6429287/)].
23. Manikkam R, Pitchai D. Catechin loaded chitosan nanoparticles a novel drug delivery system for cancer- synthesis and in vitro and in vivo characterization. *World J Pharm Sci*. 2014;**2**:1553-77.
24. Hosseinian Z, Rasouli R, Azarnoosh A, Mortazavi M, Akbarzadeh A. Evaluation of magnetic nanoparticles loaded with cisplatin Performance on breast cancer in In vivo and in vitro studies. *N Cell Mol Biotechnol J*. 2015;**5**(20):29-36.
25. Soetaert F, Korangath P, Serantes D, Fiering S, Ivkov R. Cancer therapy with iron oxide nanoparticles: Agents of thermal and immune therapies. *Adv Drug Deliv Rev*. 2020;**163-164**:65-83. doi: [10.1016/j.addr.2020.06.025](https://doi.org/10.1016/j.addr.2020.06.025). [PubMed: [32603814](https://pubmed.ncbi.nlm.nih.gov/32603814/)]. [PubMed Central: [PMC7736167](https://pubmed.ncbi.nlm.nih.gov/PMC7736167/)].
26. Ahn S, Seo E, Kim K, Lee SJ. Controlled cellular uptake and drug efficacy of nanotherapeutics. *Sci Rep*. 2013;**3**:1997. doi: [10.1038/srep01997](https://doi.org/10.1038/srep01997). [PubMed: [23770621](https://pubmed.ncbi.nlm.nih.gov/23770621/)]. [PubMed Central: [PMC3683668](https://pubmed.ncbi.nlm.nih.gov/PMC3683668/)].